# High-Resolution 4D Imaging in Live Cells

**Maya Shamir and Daniel Kaganovich**

*Department of Cell and Developmental Biology, Alexander Silberman Institute of Life Sciences, Hebrew University of Jerusalem, Jerusalem, Israel*

*The technological sophistication of microscopy approaches has grown by leaps and bounds over the past decade. This has yielded microscopes capable of greater sensitivity, faster acquisition, and higher resolution, as well as fluorophores and imaging tools that demonstrate more and more diversity of properties and applications. Yet for all the putative improvements to the cell biologists' tool kit, the application of potentially invaluable tools to unsolved scientific problems is still in its infancy. The purpose of our review is to discuss important innovations in live-cell imaging, focusing on practical considerations for probing biological systems at the molecular level while remaining rooted in a live-cell context.*

## 1 INTRODUCTION

The central challenge of cell biology in the current age is to integrate the reductionist, atomistic view of biological function propounded by biochemists into a holistic, qualitative analysis of cellular function and viability. At the most basic level, this requires a technological shift in experimental approaches that bridges several length and timescales of molecular organization. On one hand, to ask questions about the function of subcellular components (nucleic acids, lipids, proteins, etc.), we need to assay their molecular properties (size, shape(s), mobility, and interactive affinities) in relative isolation. On the other hand, mounting evidence of the substantial differences between the test tube and the crowded, sticky, inhomogeneous, and spatially confined intracellular environment compels us to incorporate techniques that assay events at the atomic scale into live-cell experimental systems. What this means, practically speaking, is that imaging approaches that have traditionally been used on the microscale to make qualitative observations (is the cell alive or dead?, is a specific protein expressed?, where is it localized?) must now be refined to operate on the nanoscale, bringing biochemical questions into living cells (do two proteins interact?, what is the spatiotemporal distribution of a network of proteins and how is it regulated?, what molecular events affect cellular function and health?). In discussing the improvements in live-cell imaging approaches that have begun to make these types of multiscale *in-vivo biochemistry* experiments possible, we would like also to cast an eye toward the changing paradigm of protein biochemistry and biophysics. In this new paradigm of intracellular biochemistry, concentration becomes a variable property of specific nanoenvironments; protein–protein interactions can be established by assaying probabilities from statistical distributions of observables; 'structure' refers to an ensemble of different conformational states; and the biochemical properties of a protein are subpopulation-specific.

In this article, we will discuss a number of established techniques and new innovations pertaining to the types of molecular and cell biological events, which we can now measure in living cells. We have divided our discussion of live-cell imaging into three overlapping sections: *resolution* (measuring the subcellular distribution and dynamics of proteins in a cell); *interaction* (measuring protein–protein association in living systems); and *function* (assaying protein function in living cells). As live-cell imaging approaches have evolved, it has become possible and desirable to simultaneously obtain images from the entire sample along all three axes: *x*, *y*, and *z*. With the added dimension of time, the state of the art for live-cell imaging is now to acquire the complete set of voxels for a sample (a 3D image) over time – rendering the data a 3D time-lapse, or *4D image*. This added resolution is essential for the types of measurements mentioned above and is described in detail in this article. Given the wide availability of informative, in-depth articles and reviews on many of the live-cell imaging approaches that we discuss, we have tried to narrow our focus to techniques that can be robustly and practically integrated with 3D time-lapse imaging in live samples, or *4D imaging*.

## 2 FLUORESCENCE IN LIVE SYSTEMS (RESOLUTION)

### 2.1 What to Image: Ideal Model Systems for 4D Imaging

Live-cell imaging, for the most part, means imaging using visible light (see **Fluorescence Imaging**). For this reason, transparent model organisms such as the nematode, *Caenorhabditis elegans*, the Zebrafish, *Danio rerio*, and the Baker's Yeast, *Saccharomyces cerevisiae*, have always been a favorite for live-cell imaging. Detailed cell biology experiments, however, were often left for cultured cells, owing to their relatively large size and relative flatness. Today, these classical model systems are getting a second look as ideal platforms for combining the awesome power of yeast genetics,[1] the experimental transparency of *C. elegans*, and the transparent window into the development of the vertebrate *D. rerio*, with recent improvements in imaging throughput, resolution, and sensitivity.[2,3] Using these powerful systems as the basis for in vivo biochemistry carries with it the reward of incorporating their unique advantages into the 4D imaging application. There are several notable examples. High-throughput, high-content imaging now enables full-genome investigation of microscopic phenotypes in yeast.[4] Four-dimensional imaging of *C. elegans* at high resolution enables the study of tissue-specific cells, such as neurons, in a functional multicellular organism. Long-term noninvasive imaging of Zebrafish allows for the study of organ development and function in unprecedented mechanistic detail.[3]

### 2.2 How to Image: Detecting Proteins in Live Cells

Traditional immunofluorescence techniques have been indispensable to track proteins in fixed cells, but present obstacles for experiments in live cells owing to the extensive treatments the cells must undergo before the immunoreactive proteins can be visualized. Immunofluorescence experiments are easy to carry out in a vast array of cell lines, without need to transfect or genetically modify the cells. There are many available immune-reactive fluorescent probes, suited for diverse needs of the exact cell line and experiment (see **Fluorescence Imaging**). On the other hand, the fixation process drastically perturbs delicate cellular structures and may cause artifacts in the image owing to cross-reactivity. In addition, the primary and secondary antibody complex is quite large, especially relative to a small protein of interest. The fluorescence amplification effect due to the antibody chain can distort the original protein amount. For these reasons and many others, cell biologists increasingly appreciate the advantages of live imaging over immunofluorescence. Without fluorescent antibodies, genetically engineered fluorescent fusion proteins are essential for visualizing live-cell components.

Most biologically relevant molecules are nonfluorescent, or fluoresce very dimly, creating a homogeneous background. In order to track a specific population of proteins while imaging, the protein must be attached to a fluorescent moiety. The discovery of the green fluorescent protein (GFP) revolutionized the very essence of research approaches in many biological fields. Originating in the jellyfish *Aequorea Victoria*, the gene was cloned and expressed heterologously in many different organisms, emitting a bright fluorescent signal in response to a variety of light sources. These initial experiments indicated that the gene is self-sufficient in that it carries all the necessary information for fluorescence, without the aid of jellyfish-specific chaperones, but with requirement for $O_2$ in the maturation process.[5] This finding opened a world of possible applications: GFP can be genetically fused with proteins to produce chimeras; many of these can maintain their native biological function and localization despite the fusion. Shortly following the adoption of GFP as a staple of cell biological analysis, several additional spectral variants were created, while the initial protein was improved.[6] Today there are dozens of spectral variants that can meet different experimental needs with versatility and enable multi-color labeling of different cellular components. When picking the appropriate set of fluorophores for a live-cell

**Table 1** Comparison of selected available fluorescent proteins

| Name of fluorescence probe | Advantages | Disadvantages |
| --- | --- | --- |
| EGFP | Photostable, bright, appropriate for two-color imaging with mCherry | Hard to do multicolor, partial overlap with blue fluorophores |
| mCherry | Photostable, bright, appropriate for two-color imaging with EGFP | Hard to do multicolor without good spectral detectors to distinguish other red fluorophores (e.g. E2-crimson, tomato) |
| tdTomato | Very bright, a broad spectrum | Less photostable, a broad spectra, large, and bulky |
| E2-Crimson | Tissue penetration, less phototoxicity, lower background noise | Less bright |
| Cerulean | Quite bright | High background fluorescence, high energy that may harm cells, not very photostable |
| Venus | Very bright | Very close to GFP and mCherry spectra |

imaging experiment, there are a few important considerations. The usefulness of a fluorophore for cell imaging is usually the result of a combination of three parameters: its photostability (how quickly the fluorophore bleaches when activated), its quantum yield (how brightly it fluoresces), and the breadth of its excitation/emission peaks (will its fluorescence overlap with other fluorophores used in the experiment). There are a few other parameters that should be kept in mind when picking fluorophores, including maturation time (how quickly will the fluorophore mature post translationally, and fluoresce), tendency to oligomerize, and size (some fluorophores are tandem dimers).[6] In our hands, EGFP and mCherry remain two of the most useful fluorophores as they are among the most photostable, extremely bright, and have easily resolvable excitation/emission peaks, enabling two-color imaging. Three-color imaging remains somewhat of a challenge, and usually requires a compromise on some of the three parameters mentioned. The tdTomato tandem dimer is among the brightest of all fluorescent proteins, although in our hands it is less photostable than GFP and mCherry and has a very broad yellow excitation/emission spectra, making it very difficult to resolve between GFP, mCherry, and tdTomato for three-color imaging (Table 1). tdTomato is also twice as large as most other fluorophores, because it is a tandem dimer. However, the extreme brightness and broad excitation spectrum of tdTomato can be turned to advantage. Although its size makes it less preferable for detecting a functional protein (for fear that a 60-kDa fusion may disrupt mobility and function), it can be used very effectively as a marker for cellular compartments, such as the nucleus, cytosol, ER, mitochondria, and so forth.[7,8] In addition, it can be excited by the 488-nm wavelength, usually used for GFP, but will emit in a region that can be spectrally separated from GFP with a simple filter, making it a nice tool for simultaneous detection of two fluorophores in imaging or FACS experiments.

Red shifted fluorophores are of particular importance as fluorescent proteins excited by longer wavelength light provide greater tissue penetration, and the lower energy of the wavelength minimizes the potential harm, or phototoxicity, to the surrounding cellular environment. An additional benefit of far red fluorophores is the lower background noise, as living samples usually autofluoresce in the blue/green wavelength zone.[10] Recent progress in the development of red fluorescent proteins (RFPs) has yielded a number of useful tools, such as DsRed2, mStrawberry, and mPlum. For reasons mentioned earlier, an optimal fluorescent protein for in vivo imaging would have excitation and emission spectra near the infrared region, and a class of proteins with this property has recently emerged. Examples include E2-Crimson and tagRFP657, as well as iRFP, which are based on a phytochrome of a bacterial origin.[11] iRFP has been used successfully in deep-tissue imaging by photoacoustic tomography.[12] Although red shifted fluorophores are constantly being improved, so far EGFP and mCherry remain the most reliable pair.

It is important to keep in mind that fusing an additional amino acid sequence to any protein may affect its localization and biological activity. This should not discourage live-cell experiments, as appropriate controls can usually verify proper protein function and localization. Still, GFP and all its derivatives are significantly large, around 238 amino acids, and this may have unwanted steric effects. Therefore, it is highly recommended to consider the site of fusion relative to the structure and function of the protein of interest (is there an active site or targeting sequence on the N-terminus?, is one of the termini buried inside the protein core?). Owing to some of the constraints of using protein fluorophores, alternatives to GFP have always been of interest.

One such GFP alternative is the use of biarsenic reagents for site-specific protein labeling in live cells. The Tsien lab and colleagues first developed the FlAsH (Fluorescein Arsenical Helix binder) labeling technology

in 1998, which exploits the high-affinity of arsenic for thiols.[13] The system is composed of two interacting components: a 6-amino acid sequence (tetracysteine) serving as receptor domain, which can be integrated into the DNA sequence of the protein to be labeled, and a small synthetic biarsenic compound, FlAsH, that becomes fluorescent and emits green light on binding to the above-mentioned motif in a reducing environment. The amino acids composition can be substituted and elongated,[14] but the initial best fluorescence results were obtained when abundant cysteines were placed as a parallelogram in one side of an α-helix. When FlAsH is unbound to the tetracysteine, it is bound to ethane dithiol (EDT), reducing its potential toxicity in the cell, and in this state, it is virtually nonfluorescent. A competition game of affinity toward the FlAsH is played among the EDT, serving as antidote, the tetracysteine domain, which activates the fluorescence, and other adjacent thiol-pairs present in different proteins in the cell. The FlAsH–cystein bonding is covalent but reversible.

The FlAsH method has a few potential advantages over the traditional fluorescent proteins such as GFP: the protein can be visualized immediately after translation, as there is no need for a maturation process to occur; the tetracysteine tag can be easily subcloned and is small enough as to not interfere with the protein's endogenous behavior; and similar biarsenic molecules are available today that emit light in red and blue, allowing a choice of colorful labeling (ReAsH and CHoXAsH, respectively). This method was proved valuable in a variety of applications, from Forster resonance energy transfer (FRET) and single-molecule analysis to protein stability reporters and affinity purification,[15,16] and ReAsH can even be used in electron microscopy.[17] However, the FlAsH technique has its drawbacks – poor labeling specificity, cellular toxicity, and undesired palmitoylation and oxidation of the tetracysteine motif.[18] Moreover, the FlAsH reagent is relatively expensive (certainly relative to DNA-encoded fluorophores), and displays a fair bit of background fluorescence.

The development of FlAsH paved the way for the designing of similar systems, based on a nongenetically encoded fluorescent probe, targeted at a cellular localization by a fused recognition motif. The next level is the addition of a mediator, which does not fluoresce on its own, but rather binds the fluorophore to the proper location, such as a ligase. Generally, this is regarded as an enzyme-mediated labeling method and is unique in the high labeling specificity that can be achieved. In 2010, the Ting lab introduced the PRIME method (PRobe Incorporation Mediated by Enzymes), utilizing an engineered *Escherichia coli* lipoic acid ligase. The mutated ligase can bind covalently between a blue fluorophore, 7-hydroxycoumarin, and a 13-amino acids recognition motif, and proved to efficiently 'highlight' a variety of nuclear and cytosolic proteins.[18] The approaches are in their infancy but have tremendous potential. Chemical fluorophores can be engineered to emit in far-red wavelengths much more readily than protein fluorophores and to fluoresce brightly and with high photostability. The 13-amino acids long tag can be inserted anywhere in the protein (not just the N- or C-terminus), and it is a great improvement from the 30-kDa payload of a GFP or mCherry.

## 2.3 The Sample: Special Considerations for Live-Cell Imaging

Living things tend to move around, they consist of many dynamic parts, and are sensitive to damage. These are among the most important considerations for conducting live-cell imaging over time. Movement can obviously take the sample out of the field of view, but can also obscure rapid dynamic processes, and even resolution, if movement occurs on a smaller timescale than image acquisition. Prolonged imaging, especially with lower-wavelength blue light which is used to activate GFP, will result in phototoxicity by way of free radical generation. As a corollary, prolonged imaging with too high an intensity will also photobleach the fluorophore, depleting the signal. An excellent review that surveys the full scope of considerations needed to be taken into account in live-cell imaging was published by Dailey et al.[19] Finally, some live samples require specialized environmental control (such as $CO_2$, humidity, and temperature).

Sample mobility problems can be solved by adhering cells to the coverslip. This is usually easier with cultured mammalian cells, which naturally adhere strongly to a variety of matrices. This is less so the case with glass, which is ideal for high-magnification, high-resolution imaging, but coating the glass with polylysine is effective. For yeast, which do not effectively adhere to lysine, Concanavalin A is a somewhat effective adherent. A number of solutions have been devised to completely immobilize samples that tend to move around a lot, such as yeast and *C. elegans*. Agarose pads can also be used to keep cells in place, and sometimes also to flatten them.[20] The most effective solution is immobilization with microfluidic flow.[21,22] In order to control the environment, chambered glass coverslips or 35-mm glass-bottom petri dishes are ideal. Microfluidics also allow for a variety of subtle approaches to maintain and rapidly modulate the environment surrounding the sample.[21]

Minimizing phototoxicity is similarly critical for all live-cell imaging and relates to almost every aspect of the imaging approach discussed in this article. The most effective approach is to design the right imaging system (which will be further discussed subsequently) optimizing sensitivity and speed of acquisition. In some cases, it

may be necessary to compromise on the resolution and quality of the image in order to minimize exposure and photobleaching. Finally, the development of far-red fluorophores promises to help address this challenge as well, as there is less endogenous activation at these wavelengths, which are also longer.

## 2.4 The Imaging Setup: The Microscope and Coping With Challenges of 4D Imaging

In order to be useful for visualizing biological samples labeled with any of the fluorophores discussed, a microscope must have at least three components: a source of high-intensity light in a coherent wavelength (this is usually achieved by filtering the light or simply by using lasers); an objective to focus the light on the sample (ideally a PlanApo objective ensuring correction of chromatic aberration and an NA, or numerical aperture, that is as high as possible); and a way to record the light emerging from the sample (a camera, charge-coupled device (CCD), or photomultiplier (PMT) discussed later in this article). Once these basic components are at hand, an extensive process of optimization of all of them is needed. The things that must be optimized, often as a compromise between all of these related components are *spatial resolution* $(x,y,z)$, *time resolution* $(t)$ (i.e. speed of acquisition), and sensitivity.

### 2.4.1 Spatial Resolution

There are a number of factors that confound axial $(x, y)$ resolution. One issue is related to $z$ resolution: conventional microscopy (e.g. epifluorescence microscopy – and also looking through the eyepiece of any microscope) usually has a much greater axial resolution than $z$ resolution, or depth of field. The result is that $xy$ details from different parts of the $z$-section are super-imposed obscuring $xy$ structural detail. In addition, a thick (2–3 micrometer for conventional epifluorescence) depth of field obscures axial resolution with out-of-focus light, resulting from the point-spread function (PSF) of the microscope, or in other words, the optical response of the imaging system to an object in a point in space. This out-of-focus light and spherical aberration is the result of light going through the various different media that lie between the sample and the recording instrument (objective, immersion medium, sample medium, etc.). Light travels differently through these media and perturbations and refraction of the signal result in the PSF.[23]

For this '$z$ problem,' there are different ways to distinguish between light coming from different focal planes, in order to achieve a thinner 'slicing' effect. Optical sectioning takes care of two problems at once: it improves $xy$ resolution and the signal to noise ratio (SNR) by eliminating extraneous out-of-focus light, and it increases $z$ resolution by having a submicrometer depth of field. By far, the most commonly used virtual optical sectioning approach is confocality – the use of a small (or modular) aperture to restrict out-of-focus light from the detection apparatus of the imaging system (Figure 1). An advanced detection device with high sensitivity, such as electron-multiplying couple-charged device, or a PMT, is essential in recording the images and assembling them into a coherent 3D image, after proper editing. For users unfamiliar with confocal microscopes (which are
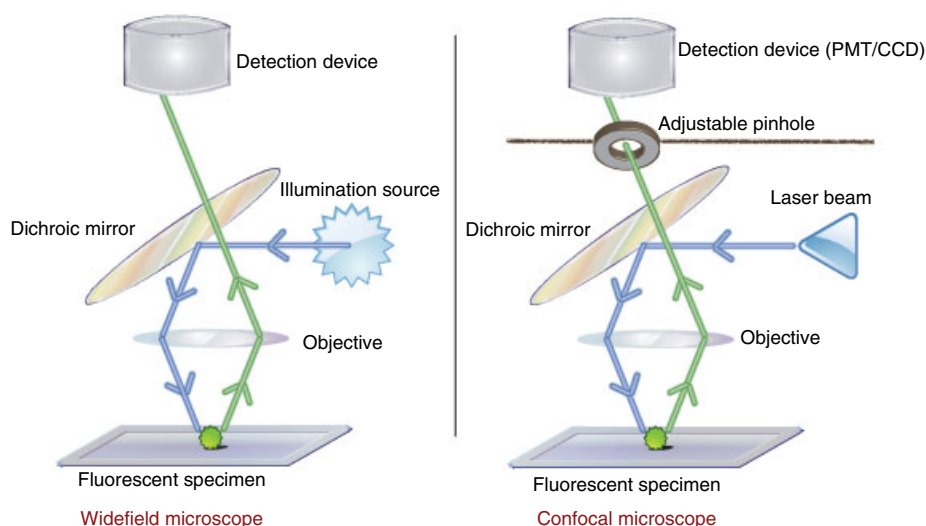


| | |
|---|---|
| Detection device | Detection device (PMT/CCD) |
| | Adjustable pinhole |
| Illumination source | Laser beam |
| Dichroic mirror | Dichroic mirror |
| Objective | Objective |
| Fluorescent specimen | Fluorescent specimen |
| **Widefield microscope** | **Confocal microscope** |

**Figure 1** Schematic structure of widefield and confocal microscopy setups. Excitation beam is shown in blue; emission beam in green. In both methods, the excitation beam is diverted by a dichroic mirror, but the emitted light from the sample is passed through. Notice the adjustable pinhole feature in confocal microscopy, which omits light coming at an angle from different focal planes.

quite widely available these days), it is important to keep in mind that the confocal pinhole is part of the detection device, not the eyepiece. When inspecting a sample by eye, before imaging, a regular halogen lamp and epifluorescence imaging is used to visualize the sample.

### 2.4.2  Time Resolution

Confocality, however, comes with its own challenges and downsides. Because a pinhole must be used in the acquisition, the sample must essentially be scanned point by point. This, of course, slows down acquisition and can lead to excess illumination (causing photobleaching and phototoxicity) as getting enough focal plane signal past the pinhole from each point requires considerable pixel-dwell for the laser.[24] This bottleneck can be resolved in a couple of ways. One is to scan multiple points simultaneously, as in spinning disk confocal microscopy. This microscope structure resembles many mini confocal systems working simultaneously on different parts of the specimen, by rotating a metal disk (Nipkow disk) spirally embedded with as many as 20,000 pinholes (Yokogawa Spinning Disk Scanning Unit). The rotational speed can reach 10,000 rpm and more, corresponding to 2000 frames per second.[25] Increasing the number of pinholes will make greater use of the available light, but eventually a 'cross-talk' between the adjacent pinholes can occur, leading to a decrease in the number of available confocal systems operating de facto. This again may be bypassed by using state-of-the-art disks with a stringent control of each pinhole opening and closing performance in perfect timing as to not interfere with its neighbors. The main advantage of the spinning disk approach is that the *rate of acquisition* is made very fast by the ability to essentially acquire the entire field of view simultaneously, and the decreased exposure time leads to the minimization of phototoxicity. Unlike point-scanning confocal instruments which usually use PMT detectors, spinning disk confocal microscopes often use CCD cameras for detection, which have higher photon efficiency (*sensitivity*). The main disadvantage of spinning disks is their decreased versatility (pinholes cannot be varied for different objectives and different sectioning parameters) and the quality of the image is generally somewhat lower than for point scanning.

There are a couple of additional alternatives to traditional (galvanometer mirror-based) point scanning that can usually acquire an image in anywhere between 0.5 and 2 s. Resonant scanners, which are mechanically and optically engineered for high-speed imaging, can perform point scanning much faster than the galvano-scanners that are generally used.[24] Resonant scanning mirrors can rival the speed of spinning disk systems (at around 30 frames per second), with most of their advantages and few of the disadvantages. As always, the increased speed comes at the cost of pixel dwell and hence, image quality. In addition, grating-based systems can use movable nanometer-sized gratings to computationally remove out-of-focus light, although this technology is fairly new to the market.

An additional confocal approach that is worth mentioning is multiphoton confocal imaging. Here, two high-wavelength photons intersect paths just at the point intended for imaging. This approach greatly increases sample penetration (as biological samples simply do not absorb at far-red wavelengths) and virtually eliminates phototoxicity and extraneous illumination of the sample.[26] There is some indication, however, that multiphoton illumination delivers a very high payload of energy at the point being imaged,[27] but otherwise this approach is extremely noninvasive over time and drastically improves SNR.

On a final note regarding confocal scanning, many of the live-cell imaging, in vivo biochemistry approaches discussed in this article can benefit tremendously from a dual-scanning system. Such a system will have one laser path continuously imaging, while another laser path is available for simultaneous laser perturbation (bleaching or photoactivation – these will be discussed in more detail subsequently).

The fourth dimension, time, may require some additional consideration. An imaging system capable of very rapid scanning of the field of view is essential, although there is an inevitable trade-off between the quality of pixel scanning and speed of acquisition. Confocal optical sectioning makes possible imaging in voxels rather than pixels (all three spatial axis, $x$, $y$, and $z$). Virtual slicing of the sample into thin layers that can be reconstructed afterward to a full volume provides essential insights into the spatial organization of the protein of interest, as intracellular components move in the $z$-direction as well as in $xy$.[28] Even when out-of-focus light is blocked by confocality, all focal planes are important for live-cell imaging because particles may go in and out of a specific $z$ plane over time. A method to acquire all of the $z$-planes is essential. For rapid imaging in $z$, piezoelectric stages offer precise and fast steps along the $z$-axis, and are essential for good temporal resolution (so that the $xyz$ acquisition does not take longer than the movement of the protein or object being imaged).

### 2.4.3  Detection Sensitivity

Since recording the data of an imaging experiment requires its conversion into a digital signal, a microscope is only as good as its ability to successfully detect as many of the (right) photons that are coming from the sample. Two major technological approaches excel at

capturing the photons very effectively: CCDs and PMTs. In choosing between them, there are two concerns that predominate: sensitivity and SNR. Sensitivity is itself a twofold question, consisting of quantum efficiency and amplification. High quantum efficiency means capturing a high percentage of the available signal.[29] Amplification takes whatever signal is available and amplifies it via the detection device. CCDs can have quantum efficiency that is up to 96%, whereas PMTs generally only go up to around 40–50% (GaAsP).[30] PMTs, however, amplify the signal much more than CCDs. PMTs work somewhat faster than CCDs and have a higher dynamic range.[31]

For multicolor imaging, an additional and somewhat orthogonal concern is spectral resolution. The standard technology for spectral resolution is to use band-pass filters to collect light in a specific wavelength range.[32] This can be done with several PMTs in parallel, enabling simultaneous multicolor imaging. Several spectral detectors, that are capable of separating wavelengths of light at very high spectral resolution, have also recently been developed. This can theoretically enable the use of fluorophores with very close emissions spectra, especially when combined with spectral unmixing.[33] A serious limitation of this approach is the decreased sensitivity of spectral detectors, which have to split the incoming light into a multitude of different paths.

Finally, an additional factor in all the considerations (mainly in spatial resolution and sensitivity) is the objective being used to capture the image. In ways that might be intuitive, the objective is the business end of the microscope, and there are a number of ways to optimize it for the type of imaging that must be done. The numerical aperture (NA) of an objective is thought to be (justifiably) one of its most important qualities. A higher NA leads to higher resolution (resolution radius = 0.6(wavelength used to image)/NA).[34] However, NA is itself a product of the medium through which the light travels (NA=(index of refraction of the objects medium)sin(half angle of light collection by the lens)). Thus, oil objectives have the highest NA (up to 1.49 for some objectives – oil breaks light more than water, hence more light reaches the objective). Water objectives, on the other hand, can have NA up to 1.27.[35] The key point, however, is that living samples usually exist in an aqueous environment. For a high NA oil objective, moving away from the oil medium for even a few micrometers will severely degrade the actual NA. Moreover, NAs of ∼1.4 and ∼1.2 are not actually huge differences in resolution. Therefore, water objectives are worth considering for live-cell imaging, where much of the sample is aqueous, and in many cases far removed from the coverslip. Water is also substantially cleaner to work with than oil, and the alignment between the immersion medium and the sample medium eliminates much of the aberration

'stretching' that is often seen in the z-axis with oil-based imaging. Objectives often come with correction collars to adjust for differences in optical thickness of the coverslip on which the sample sits. It is critical to adjust the correction collar for the actual optical thickness (not just the reported thickness) of the coverslip. Generally, it is good practice to measure the PSF with fluorescent calibration beads before imaging with a particular plate or multiwell chambered coverslip. This way, the correction collar can be adjusted to produce the appropriate point-spread function (there should be even circular rings around the beads moving out of focus in both directions (up and down)). When working with oil objectives, as is often necessary and beneficial (such as when doing total internal reflection fluorescence (TIRF) (see following paragraphs) or otherwise imaging close to the coverslip), it is important to choose an immersion oil with a refractive index that matches the objective and the coverslip. Air objectives have much lower NAs than either water or oil but can be used to seamlessly go from well to well for high-throughput imaging.[36]

## 2.5 The Special Case of Breaking the 'Resolution Limit' – Super Resolution

A rapidly emerging family of microscope technologies has been credited the name 'super resolution microscopy.' Back in 1873, Ernst Abbe realized that light microscopes have limited spatial resolution, as fundamentally derived by the light wavelength and the objective numerical aperture. As long as standard objectives and wavelengths in the visible spectrum are used (more than 400 nm to minimize harm to the cells), the uppermost lateral resolution that can be achieved with a wide-field microscope is 200 nm (see **Fluorescence Imaging Microscopy**).

This barrier seemed impassable for nearly 200 years, until the end of the twentieth century, when the first super-resolution images were obtained (Figure 2). Two methods are considered to be 'near-field,' exploiting the physical phenomenon of an evanescent wave resulting from intense illumination (laser or glass fiber). In TIRF, a ray of light is directed at the specimen's surface at an angle that is beyond the critical angle in those circumstances, resulting in total internal reflection by Snell's law. At the same time, an evanescent wave is generated but decays exponentially with distance, thus exciting only a thin layer of fluorophores that are 100–200 nm away from the original excited point. This is an artificial 'confocal' situation, with the advantage of improved axial resolution and reduced SNR, but confined to the outermost layer of the specimen closest to the glass cover.

The second method, near-field scanning optical microscopy (NSOM) scans samples with a very small,
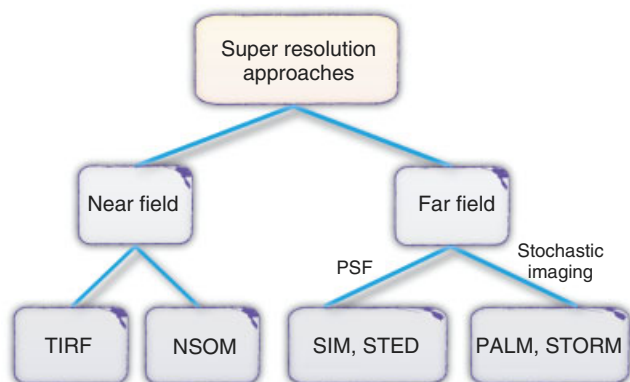
**Figure 2** Different super-resolution techniques can be divided into different subgroups, based on their general concept and operating principle. Represented here are the major super-resolution imaging techniques available today.

sharp physical aperture without any objective lenses, and generates an image that bypasses the diffraction limit in all three dimensions (20–50 nm). The near-field methods are in wide use nowadays, including research on endocytosis and exocytosis processes, but lack in ability to penetrate the cell's outer layers.

Further advancements in super-resolution provided the far-field methods, which rely on various theoretical parameters in the diffraction limit and try to attack each one (Figure 2). There are two main approaches to improving resolution further than the TIRF limit: sharpening the point-spread function and stochastic imaging or 'pointillism.' Two techniques work by sharpening the PSF, structured illumination microscopy (SIM), and stimulated emission depletion (STED). In SIM, a unique light pattern (Moire fringes) is obtained through interference of the emitted light from the specimen with a projected gridlike illumination pattern. Acquisition of multiple images of the same specimen in different orientations of the projected illumination enriches the data available to construct the image, resulting in a twofold improvement of the resolution.[37] This advancement can be further applied in 3D (3D-SIM), with more light beams producing more complex interference patterns, and enhancing the resolution an additional twofold in each dimension, all in all eightfold in comparison with traditional light microscopy.[38] In 2009, a work published by Kner et al.[39] demonstrated for the first time the relevance of SIM in super-resolution video microscopy, enabled by using a silicon spatial light modulator that reduces the speed-limiting attribute of the illumination pattern production. Ensemble techniques, such as STED, attend to the problem by modulating the excitation light to saturate the fluorophores and desaturate them in a controlled

manner.[40] The system's intrinsic attributes allow for desaturating of all fluorophores except in the very center of the beam, thereby producing a precise fluorescent spot that can be detected and analyzed so as to achieve 30–80 nm resolution.[41] SIM and STED are constantly evolving to improve resolution. Their main advantage and promise is that they are relatively fast. Live-cell imaging and super-resolution imaging are an awkward match, as any movement in the sample will translate into a devastating artifact in an imaging approach that relies on any kind of processing of raw data based on assumptions of static localization. Moreover, these and similar techniques crave photons, requiring an ever increasing amount of illumination to generate an image, thus increasing the risk of phototoxicity. That aside, new technological developments in super-resolution are promising and may enable dynamic sub-100-nm resolution of moving samples in the nearby future.

Stochastic imaging techniques can achieve much higher spatial resolution than SIM, at least at the moment. These techniques (PALM and STORM) were made possible with the development of photoactivatable dyes (PALM) and photoswitchable dye pairs or proteins (STORM), creating a system in which light can control fluorescence of a subset of molecules instead of the whole population.[42] If the excited fluorophores in each time point are properly dispersed, in proximity not under 200 nm, then the exact localization of each one can be determined. The excited fluorophores return to ground state but excite neighboring fluorophores, thus temporally providing a series of pointillistic images that once combined, constitute an image with resolution range approaching 30 nm.[43–47] The main disadvantage of these approaches for live-cell imaging is that they are extremely slow, requiring hundreds of images to make a stochastic sampling. For now, this is essentially prohibitive when it comes to working with live samples.

# 3 APPROACHES TO STUDY PROTEIN–PROTEIN INTERACTIONS

## 3.1 Forster Resonance Energy Transfer

Forster or Fluorescent Resonance Energy Transfer is a process in which energy is transferred via long-range dipole–dipole coupling, from a donor excited fluorophore to a nearby acceptor. The energy transfer takes place only if the two components are spatially separated by no more than 10 nm. The transfer rate is inversely proportional to the sixth power of the distance between the donor and the acceptor, making the energy transfer extremely sensitive to subtle changes in the distance. The range of 1–10 nm was found relevant for most biomolecules and

their interacting associates.[48] This method can be applied to measure either intramolecular or intermolecular distances and thus gain insights into protein folding or protein–protein interactions (see **Amyloids and Protein Aggregation – Analytical Methods**).

The FRET pair should meet the following spectroscopic requirements: the donor fluorophore should be sufficiently exclusive in the excitation spectrum compared to the acceptor, so that the latter does not emit light independently of the FRET process; a good separation of the emission spectra of the donor and the acceptor, so as to distinguish each of them and measure the extent of the FRET; and a partial overlap (>30%) of the donor's emission spectrum and the acceptor's excitation spectrum, to allow for FRET.[49] Excessive spectral overlap will result in significant background fluorescence, also referred to as spectral bleed-through (SBT), and careful calibration, correction methods, and wise choice of fluorophore pairs are required. The most commonly used FRET pair is not only CFP/YFP but also BFP/EGFP, EGFP/mRFP1, and mTFP/mVenus.[50]

In theory, the energy transfer can be detected either by the fluorescence emission of the acceptor (called *sensitized emission*) or by disrupting the quenching effect of the donor by the, for example, acceptor photobleaching. The latter approach is highly accurate and will be elaborated further in the 'FLIM' section.

Sensitized emission can be readily imaged in live cells by most microscopy techniques.[51,52] It amounts to exciting the donor and recording emission from the acceptor. Its main caveat is that the acceptor will be excited both by the sensitized emission (coming from the donor, i.e. FRET) and by the wavelength used to excite the donor (albeit to a lesser extent). The key to false-positive-free sensitized emission FRET imaging is to be sure of the stoichiometry of the pair from the outset (for example, if the FRET pair is fused to the same protein, then there is the exact same amount of each). If stoichiometry is unknown, it is nearly impossible to know how much of the acceptor excitation is coming from the donor, and how much is coming from off-peak excitation from the donor laser. Acceptor photobleaching, on the other hand, is much more reliable. If bleaching the acceptor unquenched donor molecules and results in an increase of the green-shifted donor fluorescence, this increased fluorescence cannot come from any other source than an unquenched donor. It is important to note that the FRET experiments can yield false negatives, e.g. it is plausible that the FRET pair is in close proximity but oriented in a way that does not produce FRET.

## 3.2 Fluorescence Correlation Spectroscopy/Fluorescence Lifetime Imaging

The fluorescence of a labeled protein can provide insight into its cellular localization in the cell, its behavior under different conditions, and many of its interactions with other proteins. It is interesting that even the fluctuations of the fluorescence over time can teach us about the protein, such as the diffusion rate and kinetic parameters, and this lies in the heart of *fluorescence correlation spectroscopy* (FCS). The amplitudes of the fluctuations can also provide thermodynamic information.

In FCS, spontaneous fluorescence intensity fluctuations are measured in a microscopic detection volume and are processed to give certain properties of the protein population. While most analytical methods to calculate diffusion coefficients, for example, are founded on disturbance of an equilibrated system in an initial state and measurement of the time it takes to regain equilibrium, in FCS the system remains in steady state, whether in equilibrium or nonequilibrium. Owing to Brownian motion, spontaneous momentary fluctuations in the fluorescence of a sample can be detected, as a stochastic process. In a spatial manner, fluorescent molecules diffusing in and out of a defined subvolume will inevitably change the local concentration and thus the fluorescence emitted from that subvolume. By establishing a direct link, or autocorrelation, between the fluorescence and the concentration of the molecules, with consideration of the specific absorbance, the quantum yield of the molecule, and the laser beam intensity, one can deduce the temporal concentration dependence and the diffusion rates.[53]

Because FCS is based on averaging fluctuations, it is important that the measured particles sample should not exceed a certain limit, as an average of a large group will eventually cross out the impact of each fluctuation. Therefore the focal subvolume should include up to 1000 molecules, equivalent to a submicromolar concentration in a femtoliter volume.[54] As a result, FCS can be applied only to dilute solutions, a challenge in the densely packed, semifluid cytoplasmic milieu in the cell. Additional limitations to FCS in vivo regard the movement restrictions in a highly disordered environment, due to specific and nonspecific binding of other cellular components to the diffusing entity. FCS analysis fits observables to an assumed theoretical diffusion coefficient. In the cell, it is not always clear which particles are diffusing and which are binding to other proteins or being shuttled around by transport machinery.[1,55]

FCS has been utilized in a vast array of applications, ranging from mobility-related parameters[56] to conformational changes, sometimes in combinations with imaging techniques presented here, such as TIRF and

STED, to enhance spatial resolution. For example, FCS can be used to assess a protein's folding state, as molten globules, intermediate folding states and the final, native folding of a protein are distinguishable in their exact diffusion coefficient. FCS is useful to measure processes in a wide range of time-scales, spanning from microseconds to molecularly slow, seconds-long processes, and therefore suit a variety of proteins. However, the analysis duration extends accordingly, as there are many components taken into account in the theoretical calculations. An excellent review of in vivo and in vitro applications can be found in Ref. 53 and in Ref. 57.

*Fluorescence lifetime imaging* (FLIM) and has become a critical research tool to assess the spatial and temporal distribution of fluorophore lifetimes inside living cells. For an extensive review of all aspects of fluorescence lifetime we refer the reader to Ref. 58.

The fluorescence lifetime, $\tau$, is the average time a fluorophore spends in the excited state before returning to ground state, accompanied by the emission of a photon, and is an intrinsic property of the fluorophore independent of most external influences. The decay of the fluorescence intensity follows an exponential decay law, and the key parameter is $\tau$. The fluorescence decay time of most biological fluorophores is in the nanosecond range but may be altered in accordance with the local environment conditions: pH, temperature, calcium ions, and so on.[51]

For biological applications such as identification of FRET, FLIM is particularly useful, as the measurement is independent of local probe concentration, excitation intensity, and stoichiometry of donor and acceptor molecules. The donor's lifetime is shortened by the FRET process, which can be measured with great precision with FLIM. In addition, the SBT, which is a major hazard in FRET imaging, is avoided by FLIM owing to the sole measurement of the donor's lifetime. FLIM is restricted to live specimens, as the probe lifetime can vary unpredictably under different environmental conditions, as inevitably takes place in sample fixation.[59]

## 3.3 Fluorescence Loss in Photobleaching/Fluorescence Recovery after Photobleaching/Photoactivation

Fluorescence recovery after photobleaching (FRAP) has become a dominant technique to assess the mobility of a protein in a living cell. In FRAP, fluorescent proteins are irreversibly bleached in a defined compartment using a localized high-intensity laser beam, and the fluorescence in that area is measured over time. The basic assumption is that a highly mobile protein population will be able to regain high fluorescence level faster than that of an immobile or low-mobile protein population. It is important to note that the fluorescent proteins themselves do not recover, but rather the diffusion of new, unbleached proteins from the surrounding environment into the region of interest (ROI) is the cause of fluorescence recovery. The results are plotted on a typical curve and two main quantitative parameters can be extracted: the mobile fraction of fluorescent molecules and the rate of mobility.[60] This technique is specifically useful in the study of lateral movement of lipids in proteins in the cell plasma membrane, as in the continuity of cellular membranes and the dynamics of many cellular proteins.[61–64]

Although FRAP has become an indispensable part of the cell biology tool kit, there are a few things worth noting when applying it to 4D imaging. FRAP recovery measurements inherently rely on time-lapse imaging, but so far this has mostly been done with imaging a single *z*-plane. Thinking in terms of voxels rather than pixels, in other words, being conscious of the *z*-dimension, is important for designing FRAP experiments and analyzing the results. Confocal imaging offers the FRAP advantage of selecting a specific ROI and bleaching with high-intensity laser only in that ROI. However, it is always good to keep in mind that the intensity of the laser will always have a 100% intensity in the ROI, but will also have a much wider distribution of lower intensities in *z*, coming in and out of the ROI. Therefore, one should not be under the illusion that the only fluorophores being bleached with each high-intensity laser pulse are those in the ROI. Too much bleaching in FRAP will deplete fluorescence in the rest of the cell, and will essentially result in fluorescence loss in photobleaching (FLIP) (discussed subsequently). If the cellular fluorescence pool is depleted, there will be less fluorescent material from which to recover fluorescence in the ROI, creating an artifactually apparent lack of mobility of the sample in the ROI. The trick is to bleach as intensely and as quickly as possible, especially when FRAPing mobile samples. Dual-scanning microscopes offer the valuable advantage of enabling simultaneous bleaching and acquisition, so even in a mobile sample the bleached area will be visible and recorded before recovery takes place. As with FCS, cell biologist should be wary of computing diffusion coefficients for proteins from FRAP data by fitting the recovery curve to first- or second-order exponentials. For some samples it is fair to assume uniform diffusion, but for many cellular factors this assumption is completely invalid. This aside, FRAP, and its inversion photoactivation (PhAc), are invaluable in determining the mobility of proteins in a subcellular compartment and can be used to assay transport, solubility, and on/off rates of proteins.[8,65] For all these approaches, careful controls are needed to determine the rate of bleaching simply due to acquisition of the image, separate from the intense bleaching by the laser.

FLIP is a complementary method that assays contiguity between two compartments with respect to protein movement. FLIP differs from FRAP in that a continuous bleaching of an area some distance from the ROI depletes all mobile fluorophores in the cell, whose mobility will eventually bring them into the laser path, at some time limit. Simultaneously measuring the fluorescence in the ROI can then determine whether all or a portion of the fluorescent material in the ROI is also mobile. The off rate of the ROI fluorescence will have a relationship to how much of the fluorescence is depleted. A highly mobile population will cause rapid fluorescence loss in the ROI itself owing to the flux of bleached molecules. In contrast, no or little change in the fluorescence would suggest that the molecules in the ROI and the bleached area are separated from one another and enclosed in a distinct cellular compartment. FLIP is often used in combination with FRAP to characterize the dynamics of cellular transport and structure and can be used de facto as a control for FRAP studies.[66] Although theoretically completely immobile material in the ROI should remain fluorescent forever, in reality FLIP theoretical assumptions obtain and should be trusted only on a relatively short time-limit. As noted above, the ROI-targeted laser will have maximum intensity only in the ROI voxels but will have some fraction of that intensity in a much larger *xy*-footprint above and below the ROI. Only multiphoton FRAP/FLIP/PhAc is able to get around this problem by having a truly voxel-specific bleaching effect. Hence, on a point-scanning confocal microscope, a long-enough FLIP experiment will also deplete fluorescence in a completely immobile ROI, as some fraction of maximal laser intensity may make contact with it in other *z*-planes.

A somewhat more recent approach, which is quickly gaining momentum, represents the inverse of FRAP. Instead of bleaching the sample, which can have adverse effects on the live cells, one can control the illumination of the fluorescence through photoactivation or PhAc. The ongoing pursuit of gathering more information about the labeled protein has invigorated the development of a new class of fluorophores, collectively named photoactivatable proteins. These fluorophores, sometimes called *highlighters*,[10] can be 'turned on' to fluoresce only under specific conditions, adding a sophisticated layer of control to many experiments such as the marking of specific organelles or protein subpopulations, and then tracking them over time. An example of a photoactivatable protein is PA-GFP, which undergoes a significant increase in 488-nm fluorescence on illumination with 413-nm light. Another promising photoswitchable protein is Dendra, which can be photoconverted from green to red fluorescent state on exposure to blue light.[67] Dendra2 is an improved version of the initial Dendra, exhibiting faster maturation and brighter fluorescence both before and after the photoactivation.[68] Dendra and Dendra2 proteins were modified to be truly monomeric, as opposed to GFP and mCherry, which were derived from self-associating proteins. This important property reduces the potential contribution of the fluorophore toward the formation of artifactual protein complexes.

The ongoing efforts to extend the available palette of photoactivatable fluorescent proteins have yielded pSmOrange, in the Verkhusha laboratory in 2011.[69] This protein can be photoconverted from orange to far-red emission spectra using blue-green light, and excels in its brightness and photostability. An improved version, pSmOrange2, is now available and has even been shown to be of value in FRET experiments, on excitation from green donor fluorophores (FRET-facilitated photoswitching,[70]).The true power of photoswitchable proteins stems from the ability to track a distinct subpopulation over time, in a quantifiable manner. The considerations that needed to be taken into account when choosing a photoactivatable protein are similar to any other fluorophore (e.g. desired wavelengths and monomer) with the added aspect of the speed and efficiency of the photoconversion and the photostability of the resulting shifted fluorophore.

A divergent branch of photoactivatable proteins includes those that are photoswitchable between a fluorescent and a nonfluorescent state. Theoretically, photoswitchable proteins are distinguished from photoactivatable proteins by the ability to be repeatedly turned on and off. Practically, photoswitchable proteins can be controlled by different wavelengths, but they would overlap with the wavelength required for generating the fluorescence emission, thus creating a complicated, intertwined pattern of fluorescence and switching.

In 2011, a photoswitchable variant of GFP by the name of Dreiklang was introduced as a breakthrough in the field of reversible switchable fluorescent proteins (RSFP).[71] Dreiklang was derived from site-directed and random mutagenesis of the yellow fluorescent protein citrine, originating from GFP. Dreiklang can be switched on on radiation with light of 365 nm, switched off with 405 nm, and the fluorescence is excited at 515 nm. With a maturation half-time time of 2 h in 37°C, it might impose some limitation on in vivo experiments that require fast reaction rates, but the fluorophore can be switched five times on and off without any noticeable phototoxic effect on the cells. However, 20 cycles of switching did have a dire effect on the cells viability. Dreiklang's usefulness was demonstrated in an FRAP-like experiment, termed *fluorescence recovery after switching* (FRAS), and even in super-resolution microscopy.

### 3.4 Bimolecular Fluorescence Complementation

In addition to FRET, protein–protein interaction can be detected through protein complementation assays (PCA), in which a biological function is obtained only through interaction of separate reporter halves. Each fragment is fused to a different protein, hence an indirect method to test the interaction between the proteins. The split reporter can be any one of biological proteins functioning in a detectable manner: split β-lactamase, split-luciferase, split-ubiquitin system (relevant to cytoplasmic/membrane-compartmentalized proteins), yeast two-hybrid system, or, most useful for live-cell imaging, split fluorophores such as GFP. The latter method, which is also termed *bimolecular fluorescence complementation* (BiFC), involves the fusion of two fragments of GFP (not fluorescent by themselves) to two proteins of interest. If the two GFP fragments are brought into close proximity by virtue of an interaction between the two proteins of interest, they fold into quasi-native structure and reconstitute the fluorescence.[72] Early versions of BiFC fluorophores, such as GFP, required an incubation temperature of 30°C in order for the recombined fluorophore to achieve maturity. Advanced Venus[73] derivatives allow for experimental procedure to take place at 37°C, the optimum temperature for most mammalian cells. Another problematic implication of the synthetic fragments is the possibility of self-assembly, creating a false-positive effect, but that as well was resolved with the development of a reduced self-assembly prone derivative of Venus.[73] BiFC has many important advantages for live-cell work, provided that controls are done to rule out self-assembly. The binary signal/no signal readout is convenient and easy to follow in living cells over time. BiFC can only detect the first successful protein–protein interaction. The maturation of the fluorophore is covalent and irreversible; therefore, this approach is less suited than FRET and others discussed for visualizing transient and on/off interactions.

## 4 REPORTERS OF PROTEIN FUNCTION

The current frontier of live-cell imaging is the visualization of localized protein function, and its modulation in living samples. This is very much a work in progress, but new sensors of stress, protein folding, and enzymatic activity are constantly coming online. When compared to global enzymatic assays as reporters of protein function, an interesting feature of fluorophores is the linearity in regard to the number of proteins expressed. While an enzymatic reaction is not strictly linear because of the abundance of the substrate, each fluorophore is fused to one protein sequence, thus the fluorescence produced can serve as a good indication of the protein expression and even functionality. However, this can be regarded as a disadvantage, as occasionally the signal propagation resulting from amplified turnover of multiple substrates aid in the observation of the protein at hand.

### 4.1 Calcium Signaling

Calcium is a central signal transduction molecule, and plays a crucial role in the metabolism and physiology of most organisms. It usually exists as a gradient across the plasma membrane, and in increased levels mediates many regulatory processes through binding to different proteins. Calmodulin is one such protein (CALcium-MODULated protein, or CaM) that transduces the calcium signal to form a biological response, through binding to different protein targets such as M13 (myosin light-chain kinase). This network of interactions was exploited to construct calcium sensors for imaging. In 1997, a fluorescent indicator was presented, consisting of two different GFP variants linked by a CaM and part of the M13 peptide chain that binds the CaM.[74] The CaM–M13 hybrid undergoes conformational change on increase in local $Ca^{2+}$ concentration, which brings closer together the two fluorophores, and FRET takes place. Alternatively, the chimera could be devised so as the binding of calcium disrupts ongoing FRET.[75] These genetically chimeric encoded $Ca^{2+}$ indicators are known as *cameleons*.[76] This method enables tracking and resolving of rapid calcium events in the cellular milieu. Furthermore, the chimeras can be directed to organelles by addition of the appropriate targeting sequences. However, problems rose as the CaM or the M13 might have undesired biological function,[5] as well as intrinsic faults in FRET sensitivity and accuracy.

A leap forward was made possible by the discovery that a single GFP could tolerate insertions of whole proteins, in the right locations in the peptide sequence.[77] The first example of a single GFP-based $Ca^{2+}$ probe was named Camgaroo1. Soon followed enhanced versions based on the same idea, of conformational changes of the GFP itself in the presence of calcium: G-CaMP[78] and pericams.[79] Instead of using two different fluorophores that undergo FRET, a single GFP which was circularly permutated was applied (cpGFP). The C′ terminal and N′ terminal of the GFP were interchanged and reconnected via a short linker. The chromophore now formed was more accessible to protons, making its electrostatic potential more prone to external changes. Once fused to CaM and M13, likewise the conformational alteration resulted in fluorescence. This chimeric protein was named 'pericam,' and several manipulations of the original molecule provided 'inverse-pericam,' in which the fluorescence

dimmed on calcium binding; and 'ratiometric-pericam,' that changed the excitation wavelength in accordance with the surrounding calcium concentration.[79] G-CaMP was later improved by introducing mutations in the cp-EGFP part as to increase the stability, brightness, and SNR, through G-CaMP1.6[80] and G-CaMP2.[9,81,82] Recently, red-shifted G-CaMP3 was demonstrated in in vivo imaging of neural circuits in various organisms.[83]

## 4.2 RedOx-Sensitive GFP

Another role for GFP derivatives as indicators is in vivo sensors of redox conditions. The cell maintains highly regulated homeostasis of redox state, which is delicately controlled in different intracellular compartments. The cytoplasm is considered a reducing environment, and rarely can disulfide bridges be found. The endoplasmic reticulum, on the other hand, is highly oxidizing, owing to its necessity in proper protein folding and function of proteins destined to be secreted. Subtle changes in the redox conditions mediate many cellular physiological responses, such as growth regulation, gene expression, metabolism, apoptosis, aging, and many more. Oxygen radicals cause protein damage and carbonylation,[84] leading to protein dysfunction and aggregation. Hence, an accurate reflection of the redox state of cellular compartments and subcompartments is highly useful for assessing health and viability. By substituting two surface-exposed residues with cysteines able to form a disulfide bond, the mutant roGFP (RedOx-sensitive GFP) alters its excitation wavelength according to the reducing/oxidizing environment. On oxidation, the chromophore increases its protonation state, and the excitation maxima is shifted from ∼490 to ∼400 nm.[85] It is important to note that the redox-reactive groups change the fluorophore properties in a ratiometric manner that is not influenced by the probe concentration, the illumination stability, excitation light path, and other distorting factors. Another major advantage over previous chemical indicators is that roGFP is genetically encoded, making it amenable to molecular engineering and targeting specific organelles according to the biological question in hand.[86] For extensive review of available roGFPs and their variants, as well as their molecular properties we refer the reader to Ref. 87. It is also extremely rapid and very sensitive. With a dual color imaging system (two PMTs for example) the ratiometric view can be acquired in real time, enabling high temporal resolution of redox changes in the cell. roGFP was used extensively to measure the oxidative state in several intracellular compartments under different conditions, such as the mitochondria and the ER.

Other similar reporters based on GFP have also been used to measure pH,[88] ER stress,[89] and apoptotic signaling[90] in the cell. Recently, an archaerhodopsin mutant was developed for real-time voltage sensing in live cells.[91] Its submillisecond response time and far-red emission spectrum hold a lot of potential for real-time visualization of action potentials in subneuronal distances, and for visualizing voltage changes in other voltage-sensitive cells. Another study devised a subtle strategy for measuring protein stability in cells by exploiting the different maturation times of EGFP and mCherry.[92] Finally, it is now possible to track individual mRNAs in live cells, by inserting a protein-binding loop.[93]

## 4.3 Folding Sensors

Proper protein folding is essential to all living things and functional proteins. Hence, the ability to assay the folding state of the cell, globally or locally, is important for any assessment of the cell's biology. A number of reporters have been generated, mostly exploiting the fact that marginally stable proteins, such as thermosensitive (ts) mutants and thermosensitive luciferase, have a lower threshold for misfolding than normal natively folded proteins. Therefore, when the protein folding homeostasis (or proteostasis) of the cell is perturbed, ts mutants and luciferase misfold first, lose solubility, and can be detected in aggregates of proteins in the cell. Proteostasis sensors have been successfully utilized in a variety of model systems including yeast,[8] C. elegans,[94] and mammalian cells.[95] These reporters (including Ubc9[ts], Ras[ts], Myo[ts], and LUC) can only report on the global state of proteostasis in the cell, as their aggregation is a secondary effect of a global decline. Very recently, an exciting study generated local real-time reporters of misfolding, but making a GFP–mCherry FRET pair on a ts protein, PGK.[96] Since the donor and acceptor were on the N- and C-termini of the protein, respectively, and as the N- and C termini were relatively close together in the folded state, there was FRET whenever the protein was folded. The authors of the study were able to visualize local fluctuations in the folding state of PGK[ts]–FRET pair by looking for localized loss of FRET, which resulted from fluctuations in the structure causing temporary unfolding.

## 5 FUTURE RESEARCH IN LIVE-CELL IMAGING

### 5.1 Optogenetics

The reporters outlined have tremendous potential when combined with 4D imaging approaches. New reporters of
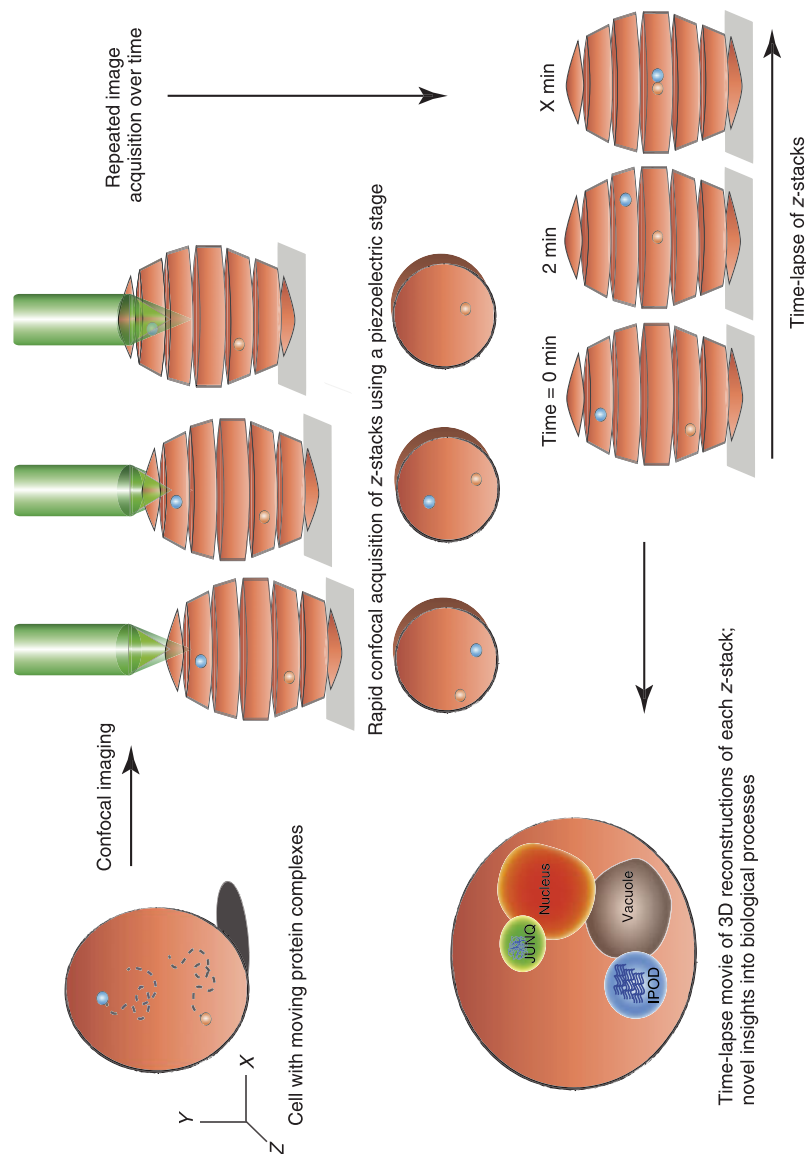
**Figure 3** 4D confocal imaging of a live specimen includes acquisition of virtual stacks over $z$-axis and over time. The $z$-axis is obtained by using a piezoelectric stage that changes the specimen's relative distance very rapidly, so that the fluorescent protein's localization at a given moment can be determined in high resolution. Repetition of this process over time allows for tracking of the protein's movement throughout the cell or the specific organelle. This technique also ensures that the entire cellular population of the protein being tracked is visible. Combining the data and rendering the images enable the visualization of processes that may be obscured from view in conventional 2D time lapse. For example, visualizing the two novel quality control compartments shown in the figure is greatly facilitated by 4D imaging. The JUNQ (juxta-nuclear quality control compartment) is the cellular quality control center where soluble aggregates from the cytosol accumulate for proteasomal degradation. The IPOD (insoluble protein deposit), which is adjacent to the vacuole, sequesters harmful aggregates and amyloids from the rest of the cytosol, thereby serving a protective function. This distinct compartmentalization is a phenomenon well conserved among eukaryotes and has major implications in many protein-aggregation-related diseases. Owing to the spherical nature of yeast, and the transient nature of certain misfolded proteins and aggregates, 4D imaging is essential for visualizing the JUNQ, nucleus, IPOD, and vacuole, which may all be in slightly different focal planes.

protein interaction and function are coming online every year. When combined with additional novel techniques for modulating cellular function, they offer insight into some of the most elusive biological processes. For example, G-CaMP and Arch imaging can be combined with the new method of optogenetics, or the ability to selectively activate or repress an action potential in a neuron by laser stimulation. Developed recently by Zhang and colleagues,[97] optogenetic channels (Channelrhodopsin, Archaerhodopsin, and others) have evolved to offer exquisite live-cell and live-animal control of neuronal activation and function. Optogenetic channels are light-sensitive and can be activated in a specific neuron or on a specific subneuronal location, by a laser pulse. They have been utilized in nearly every model system and in cell culture. Calcium sensors and voltage sensors can then be used, post activation, to visualize the action potential and signal propagation. These tools can now be combined with other reporters of protein function, cellular stress, and protein interaction. This is just one example of many emerging tools that will allow us to bridge the scale gap from the single protein to the entire cell and organism.

## 5.2 Subcellular Protein Atlas

Current imaging techniques have created an opportunity to peer into the subcellular level and attempts have been made to map out the architecture of the cell in unprecedented detail.[98] Systematic, large-scale studies of protein localizations have been carried out and their results are accessible in several databases (LocDB,[99] LOCATE,[100] and HPRD[101]). However, most of these studies involved fixation or fractionation of the cells, mostly with immunofluorescence methods. High-throughput imaging of full-genome fluorescent proteins in live cells have so far been done only in yeast[102,103] and in the nematode *C. elegans*,[104] and at relatively low resolution. Recently, some proteins in live human cells were systematically localized by labeling with YFP using a sophisticated transfection method, with the added value of the proteins dynamics characterization with time-lapse movies.[105] In the future, similar libraries assembled with 4D imaging will provide further insights into each protein function and dynamics.

## 5.3 4D Imaging in Protein Aggregation and Quality Control

Our laboratory focuses on the study of protein folding quality control and regulation, using a wide variety of tools including state-of-the-art microscopy facilities and techniques. Proteins undergo an elaborate series of modifications and folding steps to arrive at their final, functional 3D conformation. If this process is perturbed, either by a mutation that changes the primary amino
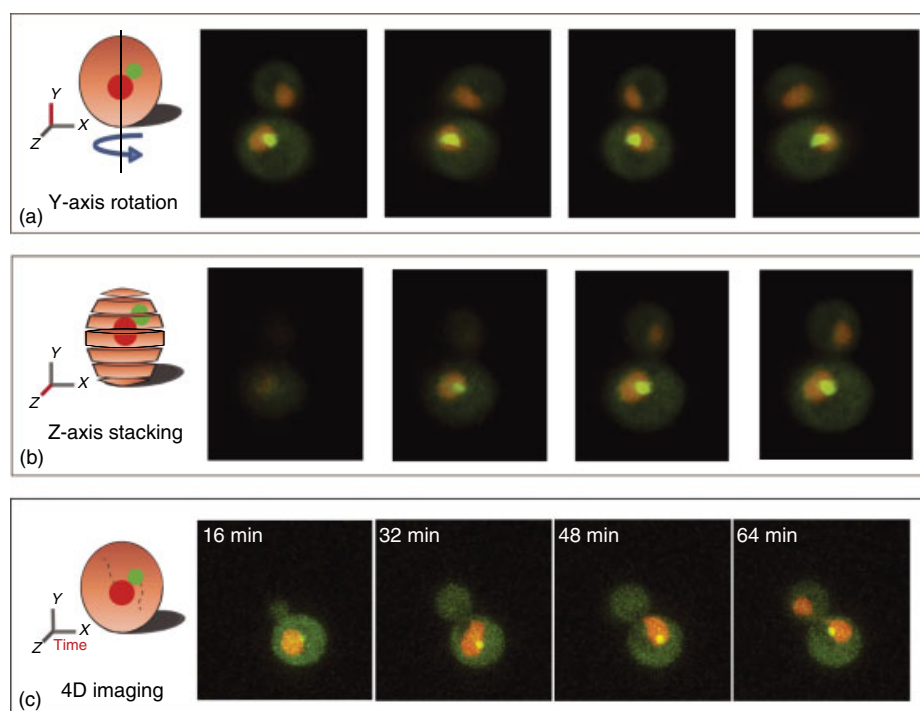


**Figure 4** Example of 4D imaging of the asymmetric inheritance of the yeast JUNQ compartment during budding. The nucleus is marked with NLS-TFP and the JUNQ is labeled with a GFP-VHL aggregate. The images were taken from Spokoini et al., Ref. 1. (Reproduced with permission from Ref. 1. Copyright 2012, Elsevier.)

acids sequence or by an environmental shift from the natural conditions that allow the folding, then quality control systems kick in to maintain cellular viability. The misfolded protein may undergo any of the following pathways: aggregation, degradation, sequestration in protective inclusions, and extensive interactions with folding chaperones. Understanding more of the cellular struggle with misfolded proteins will help shed light on many pathologies related to protein aggregates, mainly neurodegenerative diseases (e.g. Alzheimer's, Parkinson's, Huntington's). Tracing a protein population as it undergoes spatial organization and distribution over time according to its folding state and the quality control machinery is one such method to learn more (Figure 3). With some of the methods presented earlier, including confocal and super-resolution microscopy, we have been able to observe an asymmetric inheritance phenomenon that characterizes stress foci formed by misfolded proteins in the yeast cell in great detail (Figure 4).[1] This is a regulated process that actively ensures misfolded, harmful proteins are retained in the mother cell and are not passed on to the next generation. This study helps clarify the importance of aggregation compartmentalization in eukaryotic cells, and with further advancement in resolution and microscopy applications, may help understand more about protein dynamics in health and disease.

## ABBREVIATIONS AND ACRONYMS

| | |
|---|---|
| BiFC | Bimolecular Fluorescence Complementation |
| CCD | Charge-Coupled Device |
| FLIP | Fluorescence Loss in Photobleaching |
| FCS | Fluorescence Correlation Spectroscopy |
| FLIM | Fluorescence Lifetime Imaging |
| FRAP | Fluorescence Recovery after Photobleaching |
| FRET | Forster Resonance Energy Transfer |
| PhAc | Photoactivation |
| PMT | Photomultiplier |
| PSF | Point-Spread function |
| SIM | Structured Illumination Microscope |
| STED | Stimulated Emission Depletion |

## RELATED ARTICLES

*Biomedical Spectroscopy* **(Volume 1)**
Fluorescence Imaging

*Electronic Absorption and Luminescence* **(Volume 12)**
Fluorescence Imaging Microscopy

Amyloids and Protein Aggregation – Analytical Methods

Protein Dynamics

## REFERENCES

1. R. Spokoini, O. Moldavski, Y. Nahmias, J.L. England, M. Schuldiner, Kaganovich D., 'Confinement to Organelle-Associated Inclusion Structures Mediates Asymmetric Inheritance of Aggregated Protein in Budding Yeast', *Cell Rep.*, **2**, 738–747 (2012).

2. J. Lippincott-Schwartz, 'Imaging: Visualizing the Possibilities', *J. Cell Sci.*, **123**, 3619–3620 (2010).

3. K. Yaniv, S. Isogai, D. Castranova, L. Dye, J. Hitomi, B.M. Weinstein, 'Live Imaging of Lymphatic Development in the Zebrafish', *Nat. Med.*, **12**, 711–716 (2006).

4. N. Rimon, M. Schuldiner, 'Getting the Whole Picture: Combining Throughput with Content in Microscopy', *J. Cell Sci.*, **124**, 3743–3751 (2011).

5. R.Y. Tsien, 'The Green Fluorescent Protein', *Annu. Rev. Biochem.*, **67**, 509–544 (1998).

6. N.C. Shaner, M.Z. Lin, M.R. McKeown, P.A. Steinbach, K.L. Hazelwood, M.W. Davidson, R.Y. Tsien, 'Improving the Photostability of Bright Monomeric Orange and Red Fluorescent Proteins', *Nat. Methods*, **5**, 545–551 (2008).

7. S.J. Weisberg, R. Lyakhovetsky, A.C. Werdiger, A.D. Gitler, Y. Soen, D. Kaganovich, 'Compartmentalization of Superoxide Dismutase 1 (SOD1G93A) Aggregates Determines Their Toxicity', *Proc. Natl. Acad. Sci. U.S.A.*, **109**, 15811–15816 (2012).

8. D. Kaganovich, R. Kopito, J. Frydman, 'Misfolded Proteins Partition Between Two Distinct Quality Control Compartments', *Nature*, **454**, 1088 (2008).

9. R.L. Strack, R.J. Keenan, B.S. Glick, 'Noncytotoxic DsRed Derivatives for Whole-Cell Labeling', *Methods Mol. Biol.*, **699**, 355–370 (2011).

10. J. Zhang, R.E. Campbell, A.Y. Ting, R.Y. Tsien, 'Creating New Fluorescent Probes for Cell Biology', *Nat. Rev. Mol. Cell Biol.*, **3**, 906–918 (2002).

11. G.S. Filonov, K.D. Piatkevich, L.-M. Ting, J. Zhang, K. Kim, V.V. Verkhusha, 'Bright and Stable Near-infrared Fluorescent Protein for In Vivo Imaging', *Nat. Biotechnol.*, **29**(8), 757–761 (2011). doi: 10.1038/nbt.1918.

12. G.S. Filonov, A. Krumholz, J. Xia, J. Yao, L.V. Wang, V.V. Verkhusha, 'Deep-tissue Photoacoustic Tomography of a Genetically Encoded Near-infrared Fluorescent Probe', *Angew. Chem.* (International edition in English), **51**(6), 1448–1451 (2012). doi: 10.1002/anie.201107026.

13. B.A. Griffin, S.R. Adams, R.Y. Tsien, 'Specific Covalent Labeling of Recombinant Protein Molecules Inside Live Cells', *Science*, **281**, 269–272 (1998).

14. B.R. Martin, B.N. Giepmans, S.R. Adams, R.Y. Tsien, 'Mammalian Cell-based Optimization of the Biarsenical-binding Tetracysteine Motif for Improved Fluorescence and Affinity', *Nat. Biotechnol.*, **23**, 1308–1314 (2005).

15. T. Machleidt, M. Robers, G.T. Hanson, 'Protein Labeling with FlAsH and ReAsH', *Methods Mol. Biol. (Clifton, NJ)*, **356**, 209–220 (2007).

16. Z. Ignatova, L.M. Gierasch, 'Monitoring Protein Stability and Aggregation *InVivo* by Real-time Fluorescent Labeling', *Proc. Natl. Acad. Sci. U.S.A.*, **101**, 523–528 (2004).

17. G. Gaietta, T.J. Deerinck, S.R. Adams, J. Bouwer, O. Tour, D.W. Laird, G.E. Sosinsky, R.Y. Tsien, M.H. Ellisman, 'Multicolor and Electron Microscopic Imaging of Connexin Trafficking', *Science*, **296**, 503–507 (2002).

18. C. Uttamapinant, K.A. White, H. Baruah, S. Thompson, M. Fernandez-Suarez, S. Puthenveetil, A.Y. Ting, 'A Fluorophore Ligase for Site-specific Protein Labeling Inside Living Cells', *Proc. Natl. Acad. Sci. U.S.A.*, **107**, 10914–10919 (2010).

19. M.E. Dailey, E. Manders, D.R. Soll, M. Terasaki. ''Confocal Microscopy of Living Cells'', in *Handbook of Biological Confocal Microscopy*, 3rd edition, ed. J.B. Pawley, Plenum, New York, 2006.

20. S.L. Fleming, C.L. Rieder, 'Flattening Drosophila Cells for High-resolution Light Microscopic Studies of Mitosis In Vitro', *Cell Motil. Cytoskel.*, **56**, 141–146 (2003).

21. P. Rosa, S. Tenreiro, V. Chu, T.F. Outeiro, J.P. Conde, 'High-throughput Study of Alpha-synuclein Expression in Yeast Using Microfluidics for Control of Local Cellular Microenvironment', *Biomicrofluidics*, **6**, 14109–141099 (2012).

22. N. Chronis, M. Zimmer, C.I. Bargmann, 'Microfluidics for In Vitro Imaging of Neuronal and Behavioral Activity in Caenorhabditis Elegans', *Nat. Methods*, **4**, 727–731 (2007).

23. J.W. Lichtman, J.A. Conchello, 'Fluorescence Micro scopy', *Nat. Methods*, **2**, 910–919 (2005).

24. D.J. Stephens, V.J. Allan, 'Light Microscopy Techniques for Live Cell Imaging', *Science*, **300**, 82–86 (2003).

25. T. Wilson, 'Spinning-disk Microscopy Systems', *Cold Spring Harb. Protoc.*, **2010**, 1208–1213 (2010).

26. R. Yuste, 'Fluorescence Microscopy Today', *Nat. Methods*, **2**, 902–904 (2005).

27. K.G. Heinze, S. Costantino, P. De Koninck, P.W. Wiseman, 'Beyond Photobleaching, Laser Illumination Unbinds Fluorescent Proteins', *J. Phys. Chem., B*, **113**, 5225–5233 (2009).

28. C. Fink, F. Morgan, L.M. Loew, 'Intracellular Fluorescent Probe Concentrations by Confocal Microscopy', *Biophys. J.*, **75**, 1648–1658 (1998).

29. G. Ball, R.M. Parton, R.S. Hamilton, I. Davis, 'A Cell Biologist's Guide to High Resolution Imaging', *Methods Enzymol.*, **504**, 29–55 (2012).

30. T.Y. Saito, E. Bernardini, D. Bose, M.V. Fonseca, E. Lorenz, K. Mannheim, R. Mirzoyan, R. Orito, T. Schweizer, M. Shayduk, M. Teshima, 'Very High QE HPDs with a GaAsP Photocathode for the MAGIC Telescope Project', *Nucl. Instrum. Methods Phys. Res., Sect. A*, **610**, 258–261 (2009).

31. J.A. Conchello, J.W. Lichtman, 'Optical Sectioning Microscopy', *Nat. Methods*, **2**, 920–931 (2005).

32. T. Zimmermann, J. Rietdorf, R. Pepperkok, 'Spectral Imaging and Its Applications in Live Cell Microscopy', *FEBS Lett.*, **546**, 87–92 (2003).

33. Y. Garini, I.T. Young, G. McNamara, 'Spectral Imaging: Principles and Applications', *Cytometry A*, **69**, 735–747 (2006).

34. D.W. Piston, 'Choosing Objective Lenses: The Importance of Numerical Aperture and Magnification in Digital Optical Microscopy', *Biol. Bull.*, **195**, 1–4 (1998).

35. M. Abramowitz, K.R. Spring, H.E. Keller, M.W. Davidson, 'Basic principles of Microscope Objectives', *Biotechniques*, **33**, 772–774, 776–778, 780–771 (2002).

36. G. Sluder, J.J. Nordberg, 'Microscope Basics', *Methods Cell Biol.*, **72**, 1–10 (2003).

37. M.G. Gustafsson, L. Shao, P.M. Carlton, C.J. Wang, I.N. Golubovskaya, W.Z. Cande, D.A. Agard, J.W. Sedat, 'Three-dimensional Resolution Doubling in Wide-field Fluorescence Microscopy by Structured Illumination', *Biophys. J.*, **94**, 4957–4970 (2008).

38. L. Shao, P. Kner, E.H. Rego, M.G.L. Gustafsson, 'Super-resolution 3D Microscopy of Live Whole Cells Using Structured Illumination', *Nat. Methods*, **8**,, (2011).

39. P. Kner, B.B. Chhun, E.R. Griffis, L. Winoto, M.G. Gustafsson, 'Super-resolution Video Microscopy of Live Cells by Structured Illumination', *Nat. Methods*, **6**, 339–342 (2009).

40. A. Punge, S.O. Rizzoli, R. Jahn, J.D. Wildanger, L. Meyer, A. Schönle, L. Kastrup, S.W. Hell, '3D Reconstruction of High-resolution STED Microscope Images', *Microsc. Res. Tech.*, **71**(9), 644–650 (2008). doi: 10.1002/jemt.20602.

41. L. Schermelleh, R. Heintzmann, H. Leonhardt, 'A Guide to Super-resolution Fluorescence Microscopy', *J. Cell Biol.*, **190**, 165–175 (2010).

42. G.H. Patterson, E. Betzig, J. Lippincott-Schwartz, H.F. Hess, 'Developing Photoactivated Localization Micro scopy (PALM)', *4th IEEE International Symposium on*

*Biomedical Imaging From Nano to Macro*, Washington, DC, USA 940–943, 2007.

43. I. Davis, 'The "Super-resolution" Revolution', *Biochem. Soc. Trans.*, **37**, 1042–1044 (2009).

44. M. Fernández-Suárez, A.Y. Ting, 'Fluorescent Probes for Super-resolution Imaging in Living Cells', *Nat. Rev. Mol. Cell Biol.*, **9**, 929–943 (2008).

45. C.G. Galbraith, J.A. Galbraith, 'Super-resolution Microscopy at a Glance', *J. Cell Sci.*, **124**, 1607–1611 (2011).

46. B. Huang, M. Bates, X. Zhuang, 'Super-resolution Fluorescence Microscopy', *Annu. Rev. Biochem.*, **78**, 993–1016 (2009).

47. J. Lippincott-Schwartz, S. Manley, 'Putting Super-resolution Fluorescence Microscopy to Work', *Nat. Methods*, **6**, 21–23 (2009).

48. E.A. Jares-Erijman, T.M. Jovin, 'FRET Imaging', *Nat. Biotechnol.*, **21**, 1387–1395 (2003).

49. R.B. Sekar, A. Periasamy, 'Fluorescence Resonance Energy Transfer (FRET) Microscopy Imaging of Live Cell Protein Localizations', *J. Cell Biol.*, **160**, 629–633 (2003).

50. P.E. Morton, M. Parsons, 'Measuring FRET Using Time-resolved FLIM', *Methods Mol. Biol.*, **769**, 403–413 (2011).

51. Y. Chen, J.D. Mills, A. Periasamy, 'Protein Localization in Living Cells and Tissues Using FRET and FLIM', *Differentiation*, **71**, 528–541 (2003).

52. S.J. Holden, S. Uphoff, J. Hohlbein, D. Yadin, L. Le Reste, O.J. Britton, A.N. Kapanidis, 'Defining the Limits of Single-molecule FRET Resolution in TIRF Microscopy', *Biophys. J.*, **99**, 3102–3111 (2010).

53. E.L. Elson, 'Fluorescence Correlation Spectroscopy: Past, Present, Future', *Biophys. J.*, **101**, 2855–2870 (2011).

54. E. Haustein, P. Schwille, 'Fluorescence Correlation Spectroscopy: Novel Variations of An Established Technique', *Annu. Rev. Biophys. Biomol. Struct.*, **36**, 151–169 (2007).

55. J.A. Fitzpatrick, B.F. Lillemeier, 'Fluorescence Correlation Spectroscopy: Linking Molecular Dynamics to Biological Function In Vitro and *InSitu*', *Curr. Opin. Struct. Biol.*, **21**, 650–660 (2011).

56. J. Capoulade, M. Wachsmuth, L. Hufnagel, M. Knop, 'Quantitative Fluorescence Imaging of Protein Diffusion and Interaction in Living Cells', *Nat. Biotechnol.*, **29**, 835–839 (2011).

57. M. Gösch, R. Rigler, 'Fluorescence Correlation Spectroscopy of Molecular Motions and Kinetics', *Adv. Drug Delivery Rev.*, **57**, 169–190 (2005).

58. M.Y. Berezin, S. Achilefu, 'Fluorescence Lifetime Measurements and Biological Imaging', *Chem. Rev.*, **110**, 2641–2684 (2010).

59. F. Festy, S.M. Ameer-Beg, T. Ng, K. Suhling, 'Imaging Proteins In Vitro Using Fluorescence Lifetime Micro scopy', *Mol. Biosyst.*, **3**, 381–391 (2007).

60. E.A.J. Reits, J.J. Neefjes, 'From Fixed to FRAP: Measuring Protein Mobility and Activity in Living Cells', *Nat. Cell Biol.*, **3**, E145–E147 (2001).

61. M. Edidin, Y. Zagyansky, T.J. Lardner, 'Measurement of Membrane Protein Lateral Diffusion in Single Cells', *Science*, **191**, 466–468 (1976).

62. R.D. Phair, T. Misteli, 'High Mobility of Proteins in the Mammalian Cell Nucleus', *Nature*, **404**, 604–609 (2000).

63. M. Nissim-Rafinia, E. Meshorer, 'Photobleaching Assays (FRAP & FLIP) to Measure Chromatin Protein Dynamics in Living Embryonic Stem Cells', *J. Visual. Exp.: JoVE*, **52**, (2011).

64. M. Kang, C.A. Day, K. Drake, A.K. Kenworthy, E. DiBenedetto, 'A Generalization of Theory for Two-dimensional Fluorescence Recovery After Photobleaching Applicable to Confocal Laser Scanning Microscopes', *Biophys. J.*, **97**, 1501–1511 (2009).

65. J.L. England, D. Kaganovich, 'Polyglutamine Shows a Urea-like Affinity for Unfolded Cytosolic Protein', *FEBS Lett.*, **585**, 381–384 (2011).

66. H.C. Ishikawa-Ankerhold, R. Ankerhold, G.P. Drummen, 'Advanced Fluorescence Microscopy Techniques-FRAP, FLIP, FLAP, FRET and FLIM', *Molecules*, **17**, 4047–4132 (2012).

67. N.G. Gurskaya, V.V. Verkhusha, A.S. Shcheglov, D.B. Staroverov, T.V. Chepurnykh, A.F. Fradkov, S. Lukyanov, K.A. Lukyanov, 'Engineering of a Monomeric Green-to-red Photoactivatable Fluorescent Protein Induced by Blue Light', *Nat. Biotechnol.*, **24**(4), 461–465 (2006). doi: 10.1038/nbt1191.3.

68. D.M. Chudakov, S.Lukyanov, K.A. Lukyanov, 'Using Photoactivatable Fluorescent Protein Dendra2 to Track Protein Movement', *BioTechniques*, **42**(5), 553–563, (2007).

69. O.M. Subach, G.H. Patterson, L.-M. Ting, Y. Wang, J.S. Condeelis, V.V. Verkhusha, 'A Photoswitchable Orange-to-far-red Fluorescent Protein, PSmOrange', *Nat. Methods*, **8**(9), 771–777 (2011). doi: 10.1038/nmeth.1664.

70. O.M. Subach, D. Entenberg, J.S. Condeelis, V.V. Verkhusha, 'A FRET-Facilitated Photoswitching Using an Orange Fluorescent Protein with the Fast Photoconversion Kinetics', *J. Am. Chem. Soc.*, **134**(36), 14789–14799 (2012). doi: 10.1021/ja3034137.

71. T. Brakemann, A.C. Stiel, G. Weber, M. Andresen, I. Testa, T. Grotjohann, M. Leutenegger, U. Plessmann, H. Urlaub, C. Eggeling, M.C. Wahl, S.W. Hell, S. Jakobs, 'A Reversibly Photoswitchable GFP-like Protein with Fluorescence Excitation Decoupled from Switching', *Nat. Biotechnol.*, **29**, 942–947 (2011).

72. S.A. Goncalves, J.E. Matos, T.F. Outeiro, 'Zooming Into Protein Oligomerization in Neurodegeneration Using BiFC', *Trends Biochem. Sci.*, **35**, 643–651 (2010).

73. Y. Kodama, C.-D. Hu, 'An Improved Bimolecular Fluorescence Complementation Assay with a High Signal-to-noise Ratio', *BioTechniques*, **49**, 793–805 (2010).

74. A. Miyawaki, J. Llopis, R. Heim, J.M. Mccaffery, J.A. Adams, M. Ikurak, R.Y. Tsien, 'Fluorescent Indicators for Ca2+ Based on Green Fluorescent Proteins and Calmodulin', *Nature*, **388**, 882–887 (1997).

75. A. Persechini, J. Lynch, V. Romoser, 'Novel Fluorescent Indicator Proteins for Monitoring Free Intracellular Ca2+', *Cell Calcium*, **22**, 209–216 (1997).

76. K. Truong, A. Sawano, H. Mizuno, H. Hama, K.I. Tong, T.K. Mal, A. Miyawaki, M. Ikura, 'FRET-based In Vitro Ca2+ Imaging by a New Calmodulin-GFP Fusion Molecule', *Nat. Struct. Biol.*, **8**, 1069–1073 (2001).

77. G.S. Baird, D.A. Zacharias, R.Y. Tsien, 'Circular Permutation and Receptor Insertion within Green Fluorescent Proteins', *Proc. Natl. Acad. Sci. U.S.A.*, **96**, 11241–11246 (1999).

78. J. Nakai, M. Ohkura, K. Imoto, 'A High Signal-to-noise Ca(2+) Probe Composed of a Single Green Fluorescent Protein', *Nat. Biotechnol.*, **19**, 137–141 (2001).

79. T. Nagai, A. Sawano, E.S. Park, A. Miyawaki, 'Circularly Permuted Green Fluorescent Proteins Engineered to Sense Ca2+', *PNAS*, **98**, 3197–3202 (2001).

80. M. Ohkura, M. Matsuzaki, H. Kasai, K. Imoto, J. Nakai, 'Genetically Encoded Bright Ca2+ Probe Applicable for Dynamic Ca2+ Imaging of Dendritic Spines', *Anal. Chem.*, **77**, 5861–5869 (2005).

81. Y.N. Tallini, M. Ohkura, B.R. Choi, G. Ji, K. Imoto, R. Doran, J. Lee, P. Plan, J. Wilson, H.B. Xin, A. Sanbe, J. Gulick, J. Mathai, J. Robbins, G. Salama, J. Nakai, M.I. Kotlikoff, 'Imaging Cellular Signals in the Heart In Vitro : Cardiac Expression of the High-signal Ca2+ Indicator GCaMP2', *Proc. Natl. Acad. Sci. U.S.A.*, **103**, 4753–4758 (2006).

82. J. Akerboom, J.D.V. Rivera, M.M.R. Guilbe, E.C.A. Malavé, H.H. Hernandez, L. Tian, S.A. Hires, J.S. Marvin, L.L. Looger, E.R. Schreiter, 'Crystal Structures of the GCaMP Calcium Sensor Reveal the Mechanism of Fluorescence Signal Change and Aid Rational Design', *J. Biol. Chem.*, **284**, 6455–6464 (2009).

83. L. Tian, S.A. Hires, T. Mao, D. Huber, M.E. Chiappe, S.H. Chalasani, L. Petreanu, J. Akerboom, S.A. McKinney, E.R. Schreiter, C.I. Bargmann, V. Jayaraman, K. Svoboda, L.L. Looger, 'imaging Neural Activity in Worms, Flies and Mice with Improved GcamP Calcium Indicators', *Nat. Methods*, **6**, 875–881 (2009).

84. H. Aguilaniu, L. Gustafsson, M. Rigoulet, T. Nyström, 'Asymmetric Inheritance of Oxidatively Damaged Proteins During Cytokinesis', *Science*, **299**, 1751–1753 (2003).

85. G.T. Hanson, R. Aggeler, D. Oglesbee, M. Cannon, Ra. Capaldi, R.Y. Tsien, S.J. Remington, 'Investigating Mitochondrial Redox Potential with Redox-sensitive Green Fluorescent Protein Indicators', *J. Biol. Chem.*, **279**, 13044–13053 (2004).

86. C.T. Dooley, T.M. Dore, G.T. Hanson, W.C. Jackson, S.J. Remington, R.Y. Tsien, 'Imaging Dynamic Redox Changes in Mammalian Cells with Green Fluorescent Protein Indicators', *J. Biol. Chem.*, **279**, 22284–22293 (2004).

87. A.J. Meyer, T.P. Dick, 'Fluorescent Protein-based Redox Probes', *Antioxid. Redox Signal.*, **13**, 621–650 (2010).

88. V.V. Belousov, A.F. Fradkov, K.A. Lukyanov, D.B. Staroverov, K.S. Shakhbazov, A.V. Terskikh, S. Lukyanov, 'Genetically Encoded Fluorescent Indicator for Intracellular Hydrogen Peroxide', *Nat. Methods*, **3**, 281–286 (2006).

89. K. Yoshiuchi, H. Kaneto, T.A. Matsuoka, K. Kohno, T. Iwawaki, Y. Nakatani, Y. Yamasaki, M. Hori, M. Matsuhisa, 'Direct Monitoring of In Vitro ER Stress During the Development of Insulin Resistance with ER Stress-activated Indicator Transgenic Mice', *Biochem. Biophys. Res. Commun.*, **366**, 545–550 (2008).

90. N. Yivgi-Ohana, M. Eifer, Y. Addadi, M. Neeman, A. Gross, 'Utilizing Mitochondrial Events as Biomarkers for Imaging Apoptosis', *Cell Death Dis.*, **2**, e166–e166 (2011).

91. J.M. Kralj, A.D. Douglass, D.R. Hochbaum, D. Maclaurin, A.E. Cohen, 'Optical Recording of Action Potentials in Mammalian Neurons Using a Microbial Rhodopsin', *Nat. Methods*, **9**, 90–95 (2012).

92. A. Khmelinskii, P.J. Keller, A. Bartosik, M. Meurer, J.D. Barry, B.R. Mardin, A. Kaufmann, S. Trautmann, M. Wachsmuth, G. Pereira, W. Huber, E. Schiebel, M. Knop, 'Tandem Fluorescent Protein Timers for In Vitro Analysis of Protein Dynamics', *Nat. Biotechnol.*, **85**, 708–714 (2012).

93. L. Haim-Vilmovsky, N. Gadir, R.H. Herbst, J.E. Gerst, 'A Genomic Integration Method for the Simultaneous Visualization of Endogenous mRNAs and their Translation Products in Living Yeast', *RNA*, **17**, 2249–2255 (2011).

94. A. Ben-Zvi, E.A. Miller, R.I. Morimoto, 'Collapse of Proteostasis Represents an Early Molecular Event in Caenorhabditis Elegans Aging', *Proc. Natl. Acad. Sci. U.S.A.*, **106**, 14914–14919 (2009).

95. J. Hageman, M.J. Vos, M.A. van Waarde, H.H. Kampinga, 'Comparison of Intra-organellar Chaperone Capacity for Dealing with Stress-induced Protein Unfolding', *J. Biol. Chem.*, **282**, 34334–34345 (2007).

96. S. Ebbinghaus, A. Dhar, J.D. McDonald, M. Gruebele, 'Protein Folding Stability and Dynamics Imaged in a Living Cell', *Nat. Methods*, **7**, 319–323 (2010).

97. F. Zhang, L.P. Wang, E.S. Boyden, K. Deisseroth, 'Channelrhodopsin-2 and Optical Control of Excitable Cells', *Nat. Methods*, **3**, 785–792 (2006).

98. L. Barbe, E. Lundberg, P. Oksvold, A. Stenius, E. Lewin, E. Bjorling, A. Asplund, F. Ponten, H. Brismar, M. Uhlen, H. Andersson-Svahn, 'Toward a Confocal Subcellular Atlas of the Human Proteome', *Mol. Cell. Proteomics: MCP*, **7**, 499–508 (2008).

99. S. Rastogi, B. Rost, 'LocDB: Experimental Annotations of Localization for Homo Sapiens and Arabidopsis Thaliana', *Nucleic Acids Res.*, **39**, D230–D234 (2011).

100. J. Sprenger, J. Lynn Fink, S. Karunaratne, K. Hanson, N.A. Hamilton, R.D. Teasdale, 'LOCATE: A Mammalian Protein Subcellular Localization Database', *Nucleic Acids Res.*, **36**, D230–D233 (2008).

101. S. Peri, J.D. Navarro, R. Amanchy, T.Z. Kristiansen, C.K. Jonnalagadda, V. Surendranath, V. Niranjan, B. Muthusamy, T.K. Gandhi, M. Gronborg, N. Ibarrola, N. Deshpande, K. Shanker, H.N. Shivashankar, B.P. Rashmi, M.A. Ramya, Z. Zhao, K.N. Chandrika, N. Padma, H.C. Harsha, A.J. Yatish, M.P. Kavitha, M. Menezes, D.R. Choudhury, S. Suresh, N. Ghosh, R. Saravana, S. Chandran, S. Krishna, M. Joy, S.K. Anand, V. Madavan, A. Joseph, G.W. Wong, W.P. Schiemann, S.N. Constantinescu, L. Huang, R. Khosravi-Far, H. Steen, M. Tewari, S. Ghaffari, G.C. Blobe, C.V. Dang, J.G. Garcia, J. Pevsner, O.N. Jensen, P. Roepstorff, K.S. Deshpande, A.M. Chinnaiyan, A. Hamosh, A. Chakravarti, A. Pandey, 'Development of Human Protein Reference Database as an Initial Platform for Approaching Systems Biology in Humans', *Genome Res.*, **13**, 2363–2371 (2003).

102. W.K. Huh, J.V. Falvo, L.C. Gerke, A.S. Carroll, R.W. Howson, J.S. Weissman, E.K. O'Shea, 'Global Analysis of Protein Localization in Budding Yeast', *Nature*, **425**, 686–691 (2003).

103. D.Q. Ding, Y. Tomita, A. Yamamoto, Y. Chikashige, T. Haraguchi, Y. Hiraoka, 'Large-scale Screening of Intracellular Protein Localization in Living Fission Yeast Cells by the Use of a GFP-fusion Genomic DNA Library', *Genes Cells*, **5**, 169–190 (2000).

104. M. Sarov, J.I. Murray, K. Schanze, A. Pozniakovski, W. Niu, K. Angermann, S. Hasse, M. Rupprecht, E. Vinis, M. Tinney, E. Preston, A. Zinke, S. Enst, T. Teichgraber, J. Janette, K. Reis, S. Janosch, S. Schloissnig, R.K. Ejsmont, C. Slightam, X. Xu, S.K. Kim, V. Reinke, A.F. Stewart, M. Snyder, R.H. Waterston, A.A. Hyman, 'A Genome-Scale Resource for In Vitro Tag-based Protein Function Exploration in C. Elegans', *Cell*, **150**, 855–866 (2012).

105. A. Sigal, T. Danon, A. Cohen, R. Milo, N. Geva-Zatorsky, G. Lustig, Y. Liron, U. Alon, N. Perzov, 'Generation of a Fluorescently Labeled Endogenous Protein Library in Living Human Cells', *Nat. Protoc.*, **2**, 1515–1527 (2007).